Use of aligned fibers to enhance the performance of dielectric elastomer inchworm robots

Samuel Shian*, Katia Bertoldi, and David R. Clarke
School of Engineering and Applied Sciences, Harvard University,
Cambridge, Massachusetts 02138, USA

ABSTRACT

Inchworm based on the voltage actuation of dielectric elastomer actuators (DEAs) are amongst the simplest types of robots. We demonstrate a proof-of-concept inchworm robot that incorporates a few aligned fibers to suppress undesirable actuator bulging and more effectively convert the bending of a dielectric elastomer unimorph to forward motion. Finite element modeling confirms the role of the fibers in suppressing bulging but also shows that a threshold actuation voltage is required to convert the unimorph bending to forward motion of the inchworm. Based on the modeling results for unimorphs having different fiber spacing a simple inchworm is constructed and locomotion is demonstrated for actuation above the threshold voltage. Although not optimized, the inchworm illustrates the importance of using selectively positioned stiffening fibers as well as elastomers having lower viscoelastic losses.

Keywords: dielectric elastomer actuators, fiber-stiffening, bending, unimorph, soft robot

1. INTRODUCTION

The biaxial expansion of an elastomer sheet when a voltage is applied through its thickness is the basis for a number of voltage controlled dielectric elastomer actuators (DEAs). However, for several soft robotics applications mimicking the action of natural muscles such biaxial expansion is less desirable than unidirectional displacement. So to achieve, as well as optimize, unidirectional displacement, it is necessary to engineer the actuator configurations. Amongst the approaches that have been considered are to pre-strain the elastomer, impose boundary constraints as well as superimpose directional loading [1].

Pre-straining is commonly used to improve the performance of DEAs because it can suppress the pull-in instability as well as increase the electric breakdown field strength [1, 2]. Although effective, pre-straining has several practical drawbacks, including the fact that the elastomer is constantly under tensile stress and that some sort of frame is required to support and maintain the pre-strain. The existence of the tensile stress makes the elastomer membrane vulnerable to rupture from punctures or flaws [3]. The support frames needed increase the overall weight of the actuator and consequently decrease the overall power density. While the weight penalty can be minimized by using stiff materials for the frame, this reduces the overall flexibility of the system and makes it less attractive as an actuator for compatibility with other soft materials, such as tissues [4]. Together these disadvantages motivate the current study exploring the possibility of using DEAs as unimorphs in an inchworm robot without pre-strain but with a few aligned fibers.

Several groups have demonstrated bending actuators or unimorphs, consisting of a bilayer (or multilayer) of two materials, one an “active” elastomer layer actuated by an applied voltage and the other “passive” [5 – 8]. In response to an applied voltage, the active material changes dimensions, causing the unimorph to flex and exert a force. However, the elastomer response is still bi-axial. As shown by Huang et al.[9] and Lu et al.[10], the incorporation of aligned fibers can restrain the response perpendicular to the fibers and also significantly improve the actuation performance of DEAs without pre-straining. Despite these advantages, detailed studies of the role of fibers in unimorph configurations are lacking. In this paper, the use of a few aligned fibers to fabricate a stable and controlled unimorph is demonstrated

*sshian@seas.harvard.edu, phone: 1-617-496-4295; website: clarke.seas.harvard.edu

together with finite element modeling to identify necessary conditions, such as fiber concentration and voltage, for realizing unidirectional bending. These concepts are demonstrated in fabricating an inchworm based on a unimorph incorporating aligned fibers to provide both the direction of motion and enhance the movement per locomotion cycle.

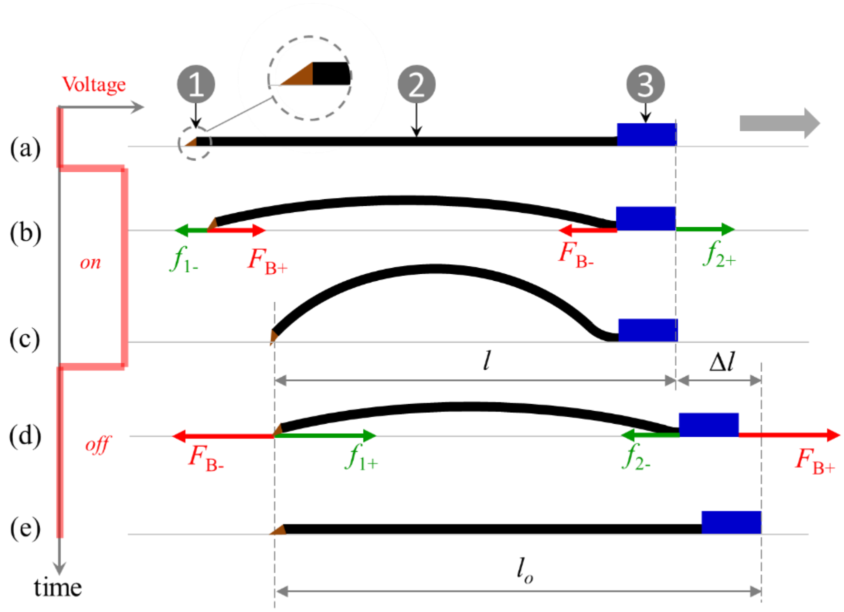

Figure 1. Schematic of the inchworm and its gait. The inchworm consists of three main parts: (1) 'tail', (2) 'body', and (3) 'head' (top). The body is a contractile unimorph actuator, while either the tail or the head or both provides anisotropic friction that give forward traction. The tail, shown as magnified inset in (a), has sharp tips placed at an angle so that the forward friction, f_{1+}, is larger than the backward friction, f_{1-}. The head friction is not anisotropic, i.e., $f_{2+} = f_{2-}$. In one gait cycle, the power supply is turned on at a constant voltage at (a). During this period, the unimorph bends from initial length, l_o, to its minimum length l and the tail moves a distance Δl. When the voltage is turned off (c), the unimorph relaxes and the head moves to the right by a distance Δl.

2. INCHWORM LOCOMOTION

The robot locomotion is based on a simplified inchworm gait, which consists of successive contraction and relaxation cycles of a bending beam. In contrast to a naturally occurring inchworm which has feet at both ends to grip surfaces and a body that has multiple degree of freedom to move in 3-D space, our design is based on a motion in one direction only. The feet are replaced with a design for anisotropic friction that biases motion in a single direction.

The robot consists of three main parts: tail, body, and head, shown schematically as part 1, 2, and 3, respectively in Fig 1a. The body is a bending actuator that contracts in the horizontal direction. Either the tail or the head or both provides anisotropic friction for forward traction. In this work, the tail has embedded sharp tips placed at an angle so that the forward friction, f_{1+}, is larger than the backward friction, f_{1-} ($f_{1+} > f_{1-}$), as shown as magnified inset in Fig 1a, where the positive and minus signs indicate the direction parallel to the net inchworm motion. Weight is added on the head to increase friction with equal magnitude in either direction ($f_{2+} = f_{2-}$). The load is adjusted so that the magnitude of head friction lies between the magnitude of forward and backward friction of the tail (i.e., $f_{1+} > f_{2+} = f_{2-} > f_{1-}$).

When the actuator is connected to a power supply, the unimorph body bends forming an arch that results in a decrease in length between the ends and produces an equal lateral force of F_{B+} and F_{B-} at both the tail and head (Fig. 1b). Because of the greater friction at the head end, i.e., $f_{1-} < f_{2+}$, the head stays still while the tail moves forward, as shown in Fig 1b. After a predetermined time, the power supply is disconnected and the body relaxes. During relaxation, the body exert equal elastic force F_{B-} and F_{B+} on both the tail and the head, respectively. Since the tail can provide larger frictional force than that on the head ($f_{1+} > f_{2-}$), the tail remains in place but the head moves forward, as shown in Fig 1d. At the end of a cycle, the unimorph body return to its original flat shape and the robot has moved forward by a distance of Δl. The speed of the robot is proportional to the cycle frequency multiplied by the distance Δl. If any slip occurs, i.e., the head slips during the contraction or the tail slips during relaxation, the effective displacement will be less than the body contraction and the speed of the robot decreases.

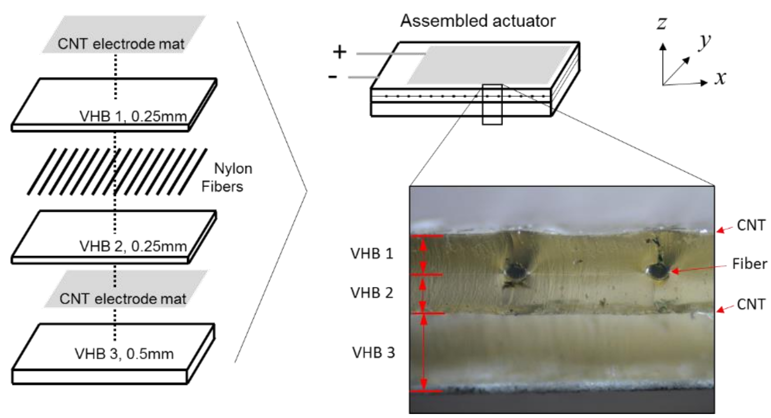

Figure 2. The bending actuator or unimorph consists of layers VHB sheets, CNT electrode mats, and nylon fiber array. An optical micrograph of 0.1 mm nylon fibers equally spaced 2 mm apart is shown in the lower right.

3. EXPERIMENTAL

The unimorph design is shown in Fig. 2. The elastomer sheets were cut from 0.25 mm and 0.5 mm thick acrylic elastomers (F9473PC and 4905 VHB, 3M) with carbon nanotubes (CNT) electrodes and a small number of aligned nylon fibers to provide unidirectional stiffening. Unlike grease or gel electrodes, solid CNT electrodes enable strong bonding between the stacked elastomer layers, eliminating slip during actuation. Details of the electrode preparation have been described previously [11] and consists of three steps as depicted in Fig. 3. Briefly, the first step was preparation of a clear dispersion of single-walled CNT in 1% SDS-water solution by tip-ultrasonication and centrifugation. Clear dispersion ensures uniform distribution of the conductive area during deposition. In the second step, an aliquot of the solution, typically 0.2 – 1 mL, was mixed with isopropanol to total volume of ~2 mL. This solution was then passed into vacuum filtration contraption that had Teflon filter (100 nm pore size and 47 mm diameter, Omnipore). The addition of isopropanol lowered the surface tension of the solution so that the solvent could easily pass the Teflon filter during vacuum filtration. This typically take less than 10 s. In the third step, the CNT mat on the Teflon filter was transferred to VHB surface by stencil masking and pressing. The mask was silicone-lined paper (4999, 3M) which was patterned using an automated paper cutter (Cameo, Silhouette America, Inc.). After firmly pressing the sheets together to ensure complete transfer of the CNT, the Teflon filter was peeled off in the presence of methanol.

The unimorph was assembled as follow; first, nylon fibers, 0.1 mm diameter, were placed in parallel to one another and sandwiched between two sheets of thin VHB (0.25mm x 50 mm long x 25 mm wide). The sheets were pressed together to bond them and the fibers together. Then, carbon nanotube electrodes, with a size of 20 mm in width and 30 mm in length, were deposited on both surfaces of the bonded sheets leaving uncoated margins of 2.5 mm along three sides and 17.5 mm along one side. The electrode area was smaller than the area of the beam so as to minimize electrical breakdown around the edges of the beam. The long uncoated side is used as a fixed end of the unimorph. Finally, the electroded sheet was attached, again under pressure, to a 0.5 mm thick VHB sheet to complete the fabrication.

An inchworm robot was fabricated by attaching ends to the unimorph in order to create anisotropic friction. Three pieces of sharp metal tips, cut from syringe needles, were attached to the rear side of robot. Additional weights using PDMS sheets were placed on the front side to increase friction there. Some modifications were made to the detailed design as will be described in section 4.2.

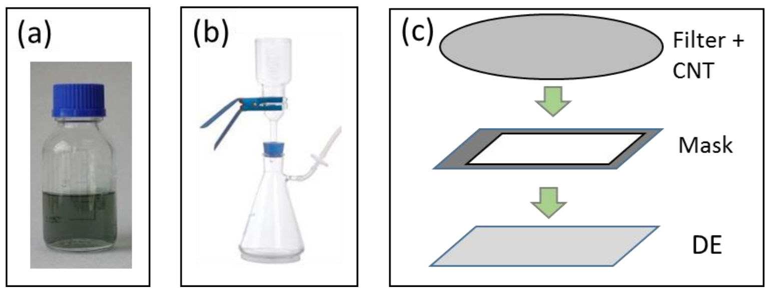

Figure 3. Three steps in the preparation of the electrode include (a) clear dispersion of CNT in 1% SDS-water solution, (b) vacuum filtration using Teflon filter, and (c) patterning and transfer using masking and pressing [11].

The actuation voltage was provided by a high voltage power supply (Model ES40P-5W-DAM, Gamma High Voltage Research, Ormond Beach, Florida) with a typical ramp rate of 300 V/s. The electro-mechanical deformation was recorded by a video camera.

Numerical simulations were performed using an electro-mechanics module in Comsol software (version 4.4, Burlington, MA). The module provides a coupling between mechanical deformations with the electrostatically-induced forces. A dielectric material ($\varepsilon_r = 4.7$) with linear elastic properties (Young's modulus, E = 0.2 MPa, and Poisson's ratio, $\upsilon = 0.49$) was assigned to the active layer. We compared the deformation of the unimorph from the simulation with experimental samples and found that the overall deformation was well captured using linear elastic assumption [2]. Fibers with linear elastic modulus of 2 GPa are placed in the middle plane the active layer and are aligned at a uniform spacing along its width direction. For simplicity, the fibers are assumed to have the same dielectric properties as the active elastomer matrix and the overall thickness of the layer is maintained. The passive elastomer layer, including the edges, has the same mechanical properties as the active layer. Mirror symmetry along the center of the unimorph, parallel to its *x* axis is implemented to shorten the calculation time. One of the short edges of the unimorph is fully constrained along a line to simulate full lateral friction. The Maxwell force is applied by defining a ground and a potential surface on opposite faces of the active elastomer layer. In this configuration, the electrodes are considered to have infinitesimal thickness and therefore to have negligible mechanical contribution to the unimorph, which is a reasonable assumption for thin CNT electrodes [11].

4. RESULTS AND DISCUSSION

In this section, the effect of fiber spacing and actuation voltage on the bending of a unimorph is first analyzed using finite element modeling. The simulations help identify conditions required for the inchworm to advance on cyclic voltage actuation and then the motion of the inchworm is demonstrated experimentally.

4.1 Finite element modeling of unimorph

The unimorphs are placed on a flat surface, where the gravitational force acts normal to the lateral surface of the unimorphs. The active side of the unimorph faced upward so that upon the application of voltage, the unimorph bends downward. One edge of the unimorph is constrained to be straight and fixed corresponding to the 'head' in the inchworm robot. Although there will be friction with the underlying surface, it is not included in the finite element model.

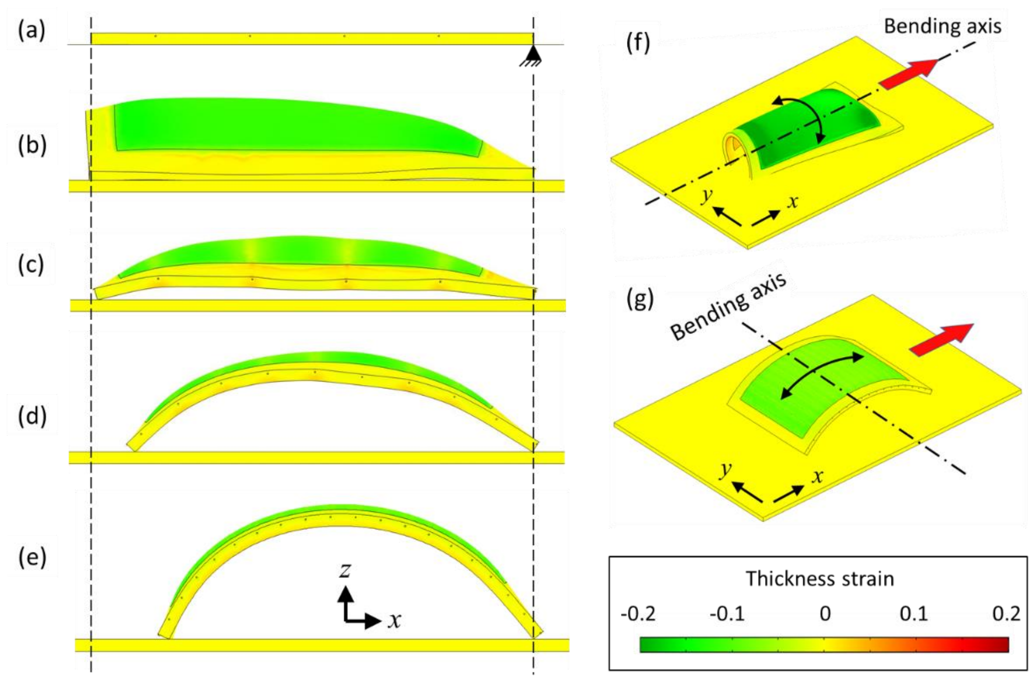

Figure 4. Finite element modeling shows the effect of the stiffening fibers on the bending deformation of the unimorph (a) at initial condition with no voltage and (b) to (g) at 12kV actuation voltage. As the number of fibers increases from (b) no fiber, (c) 8 mm, (d) 4 mm, and to (e) 2 mm spacing, the lateral length, *l*, decreases. Additionally, the bending axis changes from parallel to the forward direction (*bowing*) to become perpendicular to the forward direction (*bending*), as show in (e) and (f), respectively. The color (in online edition) indicates the magnitude of strain in the thickness direction, which mostly occur in compression mode (green color) within the electroded region.

Snapshots of the simulation of the unimorph before and after the application of 12kV with four different fiber spacing are shown in Fig 4. In all cases, the unimorph bends downward, as is expected. However the major bending axis and the amount of lateral bending differ at different fiber concentration. In the absence of fibers, the unimorph is bowing, where the bending axis of the unimorph is parallel to *x*-axis or forward direction of the unimorph, as shown in Fig 4f.

With fibers aligned in the *y*-axis or width direction, the bowing is suppressed and the bending axis along *y*-axis, parallel to the fibers, emerges. The competition between two bending axis can be seen as a progression from Fig 4b to 4e. For unimorph with 8 mm spaced fibers, bending occurs at relatively equal amount in both directions, resulting in bulging upward within the active area of the unimorph, as shown in Fig 4c. In this case, the number of fiber is not enough to provide constraint in the width direction, resulting in only 2% lateral contraction. By doubling the number of fiber, i.e., by decreasing the spacing to 4 mm, the unimorph is now able to bend mostly in the axis parallel to fiber orientation, as shown in Fig 4d. Further increase in the number of fibers provides additional increase in the bending curvature, resulting in 22% lateral contraction for 2 mm spaced fiber (Fig 4e).

The end-to-end tip displacement along the horizontal is shown as a function of actuation voltage in Fig 5 where the relative lateral contraction is calculated as: $\%\Delta l = \frac{(l-l_o)}{l_o} \times 100\%$. l_o and l are the original length and the contracted length, respectively, as shown in Fig 1. At voltages less than 10kV, the unimorphs are slightly elongated (by up to 1%), as shown by the positive lateral contraction. This elongation is caused by the biaxial lateral expansion from the Maxwell compression along the thickness of the active layer. In this low voltage regime, there is no significant difference in lateral contraction amongst the fiber-stiffened unimorphs. At high voltages, above 11 kV, negative lateral contraction or bending occurs for unimorphs with fiber stiffening, which is caused by the axial bending parallel to the width axis. Significant differences in the contraction for different fiber spacing stiffening can be seen in Fig 5. Without fibers, the lateral contraction remains positive because the bending occurs in the different axis, parallel with length of the unimorph (Fig 4f). The simulations show that a relatively low concentration of fibers, as in 2 mm spacing, is enough to force the bending in width axis.

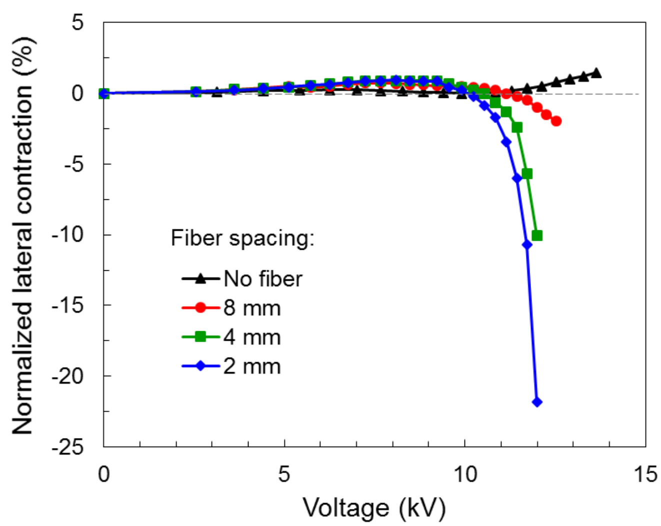

Figure 5. The voltage induced lateral contraction (l - l_o), measured between the ends of the unimorph on the surface, for the fiber spacing indicated. The contraction is normalized to the initial body length (l_o). With no fibers, the axis of the primary bending is along the length direction, which causes elongation in the length direction. With fibers the unimorphs elongate slightly at low voltages (< 10 kV) rather than contract because bending in the orthogonal direction occurs preferentially. The finite element simulation assumed no friction between the unimorph and its underlying surface

In the bimetal bending theory, the bending curvature increases monotonically with respect to the temperature-induced strain [12], which consequently should results in monotonic decrease in distance between beam tips. However, in our case, complex interplay of gravity, constraint, and edge effects contribute to the observed non-linear behavior of the lateral contraction. The simulations indicate that the power supply must exceed a threshold voltage to generate the contraction needed for forward motion of the inchworm. At or below the threshold voltage, the inchworm will not move. This threshold is caused by the presence of the two competing orthogonal bending modes, as shown in Fig 4e and 4f. Below the threshold voltage, both bending modes coexist and above the threshold, one of the bending modes dominates. In the absence of external effects such as gravity and edge constraints, the bending favors alignment with the shorter edge. For system with high elastic modulus, the alignment occurs at relatively low strain [13]. In soft unimorphs with low modulus, these external effects persist to a significantly higher strain before the bending symmetry is broken. This is reflected in the high voltage threshold. The presence of the fibers helps stabilize one of the bending modes favoring alignment with the fiber orientation. This effect can be seen in the slight decrease of threshold voltage as the number of fibers increase, e.g., threshold voltage of 11 and 10 kV for 8 mm and 2 mm fiber spacing, respectively. Above the threshold voltage, energy can be concentrated into bending in the one direction, resulting in the dramatic increase in the contraction. This is evidenced by the results shown for the unimorphs having the 4 mm and 2 mm fiber spacing in Fig 5.

4.2 Inchworm robot

Photographs of the inchworm robot are shown in Fig 6. The head consists of several layers of PDMS sheets so its weight can be adjusted by adding or removing individual sheets. The lower part of the head was deliberately curved slightly which contributes to the change in the head tilt during actuation. In this particular example, the robot body initially contained nylon fibers t 4 mm spacing, which produced little bending and resulted in sluggish performance. After adding four fibers of larger diameter than the initial fiber, the bending curvature increased and the forward speed improved. These additional fibers can be seen in Fig 6a as the dark lines, slightly shorter than the width of the inchworm. The three sharp metal tips on the tail were able to maintain traction with no observable slip during relaxation. At an actuation voltage of 17 kV, the body of the inchworm robot contracts and after the removal of voltage, the body restores to the original flat shape. At each cycle, the robot moved at approximately 3.8 mm. Thus, at 0.3 Hz actuation rate, the average speed of the robot is 1.1 mm/s, which correspond to length-specific speed of 1.3 body lengths per minute.

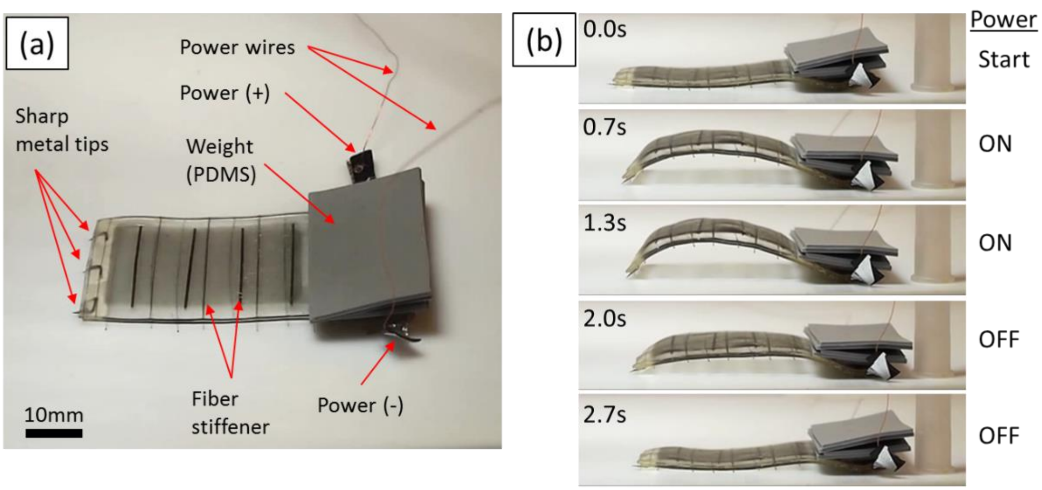

Figure 6. (a) Inchworm robot constructed from a unimorph actuator with the addition of metal tips and weight. The active electroded portion is the dark grey area, overlapping with the fibers. (b) A one-cycle sequence of the robot gait that produces a net displacement of about 3.8 mm is shown as the robot approaches a post on the right side of the frames. The voltage is set at 17 kV and 0 V at ON and OFF positions, respectively.

Other than attaching the additional four fibers mentioned above, no other attempts were made to optimize the speed of the robot so there are plenty of opportunities for further improvements. In particular, a significant portion of the rise time (~1.4 s) is needed for the power supply to reach 17kV and, during shape relaxation, the charge stored in unimorph was naturally dissipated, rather than actively removed through an external circuit. Further optimization may also include the use of anisotropic friction at the robot head so that the forward friction can be reduced and the head can move faster during relaxation in the second half of the cycle. Additionally, the load weight could be replaced with a battery and a control circuit for untethered operation.

Our experiments highlight one major shortcomings that must be overcome before elastomeric unimorphic actuators can be routinely fabricated and utilized for soft robotics; The materials selection issue. The energy density of non-pre-stretched VHB is relatively low, mainly because of its relatively low breakdown field which happen at low actuation strain. During experiments, we observed that samples were routinely breakdown at relatively low nominal field of 40 - 50 MV/m, which is far less than the maximum of 200 – 400 MV/m typically reported for pre-stretched VHB [14]. Since the stored energy is proportional to the square of electric field, such reduction in breakdown field results in the drastic drop of energy density by more than an order of magnitude. Additionally, the unimorphs should be fabricated using elastomers that exhibit little or no viscoelasticity since the inherent viscoelastic not only limits the actuation response time but also variation of modulus which affect the accuracy of the prediction. The material used in this work, the acrylic VHB was chosen because it is the easiest to work with and because it is has been the material of choice by many groups for demonstrating actuator devices over the last decade so direct comparisons between devices can be made. Evidently, though, alternatives are needed.

Despite these shortcomings, voltage actuated dielectric elastomer unimorphs show considerable potential in soft robotic applications and as illustrated by this work a very small volume fraction of aligned fibers can introduce an asymmetry in bending actuation that can result in a control of bending direction of unimorph.

5. CONCLUSIONS

The incorporation of a few aligned stiff fibers improves the bending response of unimorph actuators by suppressing two-dimensional bulging. One consequence, demonstrated in this work, is to improve the performance of inchworm robots based on voltage actuation of a dielectric elastomer actuator. In conjunction with finite element simulations, the effect of fiber spacing is illustrated and a threshold voltage identified above which inchworm motion can occur.

6. ACKNOWLEDGEMENT

This work was supported by the National Science Foundation through grant CMMI-1333835 and in part by the MRSEC program of the National Science Foundation under award number DMR 14-20570.

7. REFERENCES

[1] Anderson, I.A., Gisby, T.A., McKay, T.G., O'Brien, B.M., and Calius, E.P., "Multi-functional dielectric elastomer artificial muscles for soft and smart machines," Journal of Applied Physics 112(4), 041101 (2012).

[2] Pelrine, R., Kornbluh, R., Pei, Q., and Joseph, J., "High-speed electrically actuated elastomers with strain greater than 100%," Science 287(5454), 836–839 (2000).

[3] Pharr, M., Sun, J.-Y., and Suo, Z., "Rupture of a highly stretchable acrylic dielectric elastomer," Journal of Applied Physics 111(10), 104114 (2012).

[4] Conn, A.T., Hinitt, A.D., and Wang, P., "Soft segmented inchworm robot with dielectric elastomer muscles," Proc. SPIE 9056, 90562L (2014).

[5] Pelrine, R.E., Kornbluh, R.D., and Joseph, J.P., "Electrostriction of polymer dielectrics with compliant electrodes as a means of actuation," Sensors and Actuators A: Physical 64(1), 77–85 (1998).

[6] Lau, G.-K., Goh, S.C.-K., and Shiau, L.-L., "Dielectric elastomer unimorph using flexible electrodes of electrolessly deposited (ELD) silver," Sensors and Actuators A: Physical 169(1), 234–241 (2011).

[7] Araromi, O.A., and Burgess, S.C., "A finite element approach for modelling multilayer unimorph dielectric elastomer actuators with inhomogeneous layer geometry," Smart Materials and Structures 21(3), 032001 (2012).

[8] McGough, K., Ahmed, S., Frecker, M., and Ounaies, Z., "Finite element analysis and validation of dielectric elastomer actuators used for active origami," Smart Materials and Structures 23(9), 094002 (2014).

[9] Huang, J., Lu, T., Zhu, J., Clarke, D.R., and Suo, Z., "Large, uni-directional actuation in dielectric elastomers achieved by fiber stiffening," Applied Physics Letters 100(21), 211901 (2012).

[10] Lu, T., Huang, J., Jordi, C., Kovacs, G., Huang, R., Clarke, D.R., and Suo, Z., "Dielectric elastomer actuators under equal-biaxial forces, uniaxial forces, and uniaxial constraint of stiff fibers," Soft Matter 8(22), 6167 (2012).

[11] Shian, S., Diebold, R.M., McNamara, A., and Clarke, D.R., "Highly compliant transparent electrodes," Applied Physics Letters 101(6), 061101 (2012).

[12] Timoshenko, S., "Analysis of bi-metal thermostats," Journal of Optical Society of America 11, 233–255 (1925).

[13] Alben, S., Balakrisnan, B., and Smela, E., "Edge effects determine the direction of bilayer bending," Nano letters 11(6), 2280–5 (2011).

[14] Huang, J., Shian, S., Diebold, R.M., Suo, Z., and Clarke, D.R., "The thickness and stretch dependence of the electrical breakdown strength of an acrylic dielectric elastomer," Applied Physics Letters 101(12), 122905 (2012).